Korean J Biol Sci 1: 483-489, 1997

# Differentiation and Distribution of the Choline Acetyltransferase-immunoreactive Nerve Cells in the Magnocellular Preoptic Nucleus of the Rat Forebrains during the Postnatal Development

**Young-Wha Chung* and Yoon-Jin Choi**

*Department of Biology, Hallym University, Chunchon 200-702, Korea*

Key Words:
Nerve cell differentiation
Immunocytochemical localization
Magnocellular preoptic nucleus
Choline acetyltranseferase
Postnatal and adult rats

**This study was performed to investigate the differentiation and distribution of choline acetyltransferase (ChAT)-immunoreactive cells in the magnocellular preoptic nucleus (MCPO) of the postnatal and adult rat forebrains, utilizing techniques of immunocytochemistry. According to the cell shape and the ratio of long axis versus short axis of cell soma, the ChAT-immunoreactive nerve cells in the MCPO were classified into six types: 1) round, 2) oval, 3) elongated, 4) fusiform, 5) triangular, and 6) polygonal types. Frequency distributions of the oval and round nerve cells on the postnatal day (PND) 0 were observed to be high. But in the adult, frequency distributions of the same cells were shown to decrease. Compared to those of the postnatal rats, frequency distributions of elongated, fusiform, triangular, and polygonal nerve cells in the adult were increased. The total mean volumes of ChAT-immunoreactive cell somata in the MCPO of PND 0 rat were the lowest, while those in the PND 17 rat were shown to be the highest and decreased in the adult. The soma volumes of the immunoreactive cells at the PND 17 were evenly distributed, but those in the other developmental stages (e.g. PND 7 and adult) appeared to exhibit unimodal distributions. On the electron micrography, the free ribosomes, polysomes, and rough endoplasmic reticula (RER) of the nerve cells in the MCPO of PND 21 rat forebrains were immunoreactive to ChAT in the tissues untreated with triton X-100. According to the observations in the present study, it is considered that the ChAT-immunoreactive nerve cells in the MCPO of the rat forebrains are differentiated throughout the following processes during the postnatal development: 1) increase in cell soma volumes, 2) development of neurites, 3) increase in the frequency of differentiated cell types, and 4) decrease in cell soma volumes. The ribosomes, polysomes, and RER are considered to be closely related to the intracellular localization and biosynthesis of the ChAT but not Golgi complex.**

The cholinergic neurons, which are choline acetyltransferase (ChAT)-immunoreactive, are distributed in the brainstem and spinal cord, the somatic nerve system and the autonomic nerve system (Armstrong et al., 1983; Houser et al., 1983; McGeer et al., 1987). These neurons are known to have various functions in sleeping (Szymusiak and McGinty, 1986), memory (McGeer et al., 1981), and learning (Drachman, 1977). Those in basal forebrain are also involved in the generating and maintaining cortical activation during the state of wakefulness (Detari and Vanderwolf, 1987; Buzsaki et al., 1988) and in the initiation and maintenance of slow wave sleep (Szymusiak and McGinty, 1986; Detari and Vanderwolf, 1987).

In order to characterize the cholinergic neurons, the biochemical (Eckenstein, 1988; Dreyfus et al., 1989) and morphological methods (Armstrong, 1986; Sofroniew et al., 1987) have been utilized. The methods using radioisotope (Happe and Murrin, 1992), anterograde and retrograde tracers (Grove et al., 1986) and *in situ* hybridization using ChAT mRNA (Butcher et al., 1992; Oh et al., 1992) have been developed. Also, immunocytochemical and immunohistochemical methods using monoclonal antibody to the ChAT in the teleosts (Brantley and Bass, 1988), amphibians (Ciani et al., 1988), reptiles (Medina et al., 1993), mammals (Ko et al., 1995), and human (Mesulam et al., 1992) have been developed.

The ChAT-immunoreactive neurons are known to be

* To whom correspondence should be addressed.
Tel: 82-361-240-1433, Fax: 82-361-56-3420

distributed in the medial septal nucleus, vertical and horizontal diagonal bands of Broca, magnocellular preoptic nucleus (MCPO), ventral pallidum, and basal nucleus of Meynert in the rat forebrains (Armstrong et al., 1983; Ko et al., 1995). The MCPO, which is generally known to originate in the telencephalon, moves to the preoptic area (Bayer and Altman, 1987) and then distributes in the lateral area of the caudal part of the horizontal diagonal band of Broca. Especially, this nucleus has a complex of fibers consisting the medial forebrain bundle (Gritti et al., 1993). In addition, the ChAT-immunoreactive neurons of the MCPO and the other one of the magnocellular basal nucleus are known to project the nerve fibers to the hippocampus and neocortex, which are in charge of memory and learning functions (Koh et al., 1989; Hellweg et al., 1990).

Gould et al. (1989, 1991) have investigated the basal forebrain neurons undergoing somatal and dendritic remodeling during postnatal development. Dinopoulos (1988) identified three types of cells in the basal forebrain nuclei of the rat on the basis of soma shape and dendritic form in the Golgi-impregnated materials. Chung et al. (1994) and Ko et al. (1995) classified the nerve growth factor receptor- and the ChAT-immunoreactive nerve cells in detail into six types in the postnatal and adult rat forebrains. They also have investigated the changes of both the frequency of distributions of the cell types and their soma volumes during postnatal development. However, such observations have not been performed in the MCPO. Therefore, the present study was performed to investigate the differentiation and distribution of ChAT-immunoreactive nerve cells and their organelles in the MCPO of the postnatal and adult rat forebrains. The cell soma volumes in six cell types was also investigated at the developmental stages and the adult.

## Materials and Methods

### *Animals*

Five to six rats of Sprague-Dawley strain at the postnatal day (PND) 0, 7, 14, 17, 21, 28, 35 and 90±10 (adult) were anesthetized with sodium pentobarbital solution (5 mg/100 gm body weight) and subsequently perfused through the aorta with 0.1 M phosphate buffered saline (PBS), followed by periodate-lysine- paraformaldehyde fixative at pH 7.4 (McLean and Nakane, 1974).

### *Immunohistochemistry*

Brains were washed in 0.1 M PBS for 2 h and coronal sections were made on a vibratome (40 or 80 μm thick) throughout the rostrocaudal extent of MCPO (Paxinos and Watson, 1986). Sections were maintained in serial order for the immunocytochemical processing of ChAT. Immunocytochemical localization of ChAT was visualized with the avidin-biotin peroxidase method (Hsu et al., 1981) with recommended dilutions. Briefly, tissue sections were incubated in 0.1 M PBS containing 3% horse sera and 0.05-0.2% Triton X-100 for 1 h and incubated overnight at 4℃ with 0.5- 2.0 μg/ml of the primary antisera (monoclonal antibody against ChAT, Boehringer Mannheim) in 0.1 M PBS. The sections were washed three times in PBS for 10 min each and incubated in biotinylated horse antimouse IgG for 90 min at room temperature. After subsequent washes, sections were incubated in the avidin-biotin complex for 90 min and washed. Following the immunohistochemical procedure, sections were incubated with 3,3'-diaminobenzidine tetrahydrochloride solution containing 0.003% hydrogen peroxide for 7-10 min to visualize the reaction product at room temperature. The sections were then hydrated and coversliped. Control Sections were incubated for 16 h in PBS instead of monoclonal antibody to ChAT and were otherwise treated in the same manner.

### *Immunocytochemistry*

Immunoreacted tissue sections for ChAT were post-fixed in 1% osmium tetroxide for 1 h at 4℃ and stained *en bloc* with uranyl acetate in 70% ethyl alcohol for 2 h, dehydrated in ethyl alcohol and propylene oxide, and embedded flat in epon-araldite mixture. Selected areas were cut and remounted on blank epon blocks. Ultrathin sections were made, mounted on formvar-coated slot grids, stained with lead citrate, and observed by Zeiss EM 109.

### *Statistical analysis*

The cell types were defined by both the cell shape (triangular and polygonal) and the ratio of long axis versus short axis (round: 1.0～1.24, oval: 1.25～1.74, elongated: 1.75～2.74, fusiform: 2.75 and more). The frequency distribution was presented as a percentage (%). The volumes of the cell somata were estimated with the following equations (Dinopoulos et al., 1988): $V=(\pi/6)\times AB^2$, where A and B are the lengths of the major and minor axes, respectively, for nerve cells with round, oval, elongated, and fusiform somata and $V=(\pi/3)\times r^2 h$, where r is the radius of the base and h is the height of the pyramid for the nerve cells with triangular and polygonal perikarya.

## Results

### *Distribution and immunoreactivity of the ChAT-immunoreactive nerve cells*

In the MCPO of the postnatal and adult rats, many ChAT-immnoreactive neurons were found to be evenly distributed (Fig. 1). The boundary between the MCPO and the caudal part of horizontal band of Broca was not clearly distinctive. In the PND 0 (Figs. 1A and 3A) and 7 (Figs. 1B and 3B) rats, the nerve cells and the bundles of nerve fibers were undifferentiated and their

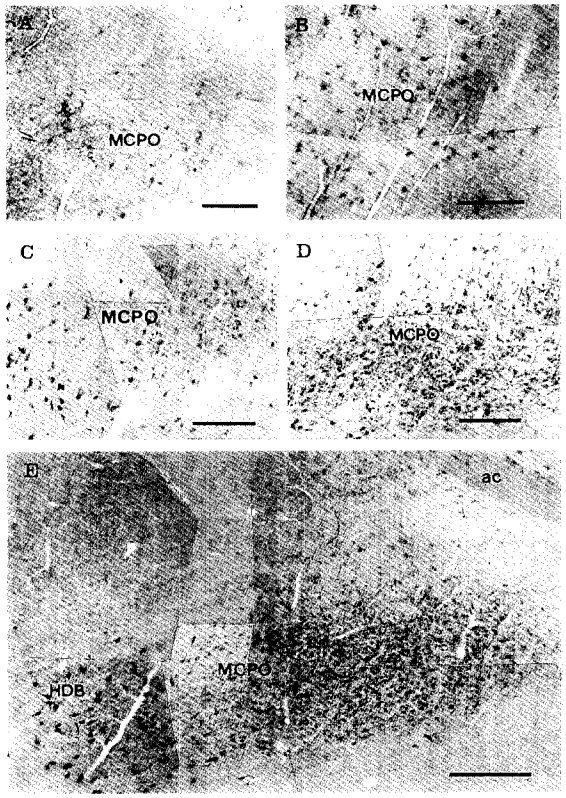


**Fig. 1.** Distribution of the ChAT-immunoreactive nerve cells in the coronal sections of the postnatal and adult rat forebrains at the anterior commisure (ac). A, A few immunoreactive nerve cells in the MCPO of the PND 0 rat. Immunoreactivity to the ChAT are considerably weak. B and C, Several immunorreactive nerve cells in the MCPOs of the PND 7 (B) and 14 (C) rats. The immunoreactivities are moderate. D and E, Many immunoreactive nerve cells in the MCPOs of the PND 35 (D) and adult (E) rats. The imunoreactivities are stronger than those in the early postnatal rats. Many immunoreactive nerve fibers are well developed. More immunoreactive nerve cells are seen in the horizontal diagonal band of Broca (HDB) than in the MCPO. Scale bars=100 μm.

immunoreactivities were weak. However, the immunoreactive nerve cells with dendrites developed in the PND 14-28 rats (Figs. 1C, 3C, and D) and their immunoreactivities were considerably intense. In the PND 35 rat (Fig. 1D), the differentiation and immunoreactivity of the immunoreactive nerve cells were similar to those of the adult rats (Figs. 1E and 3E) and many nerve fibers were also found to be well developed. Some of these fibers in the bundle showed relatively intense immunoreactivity.

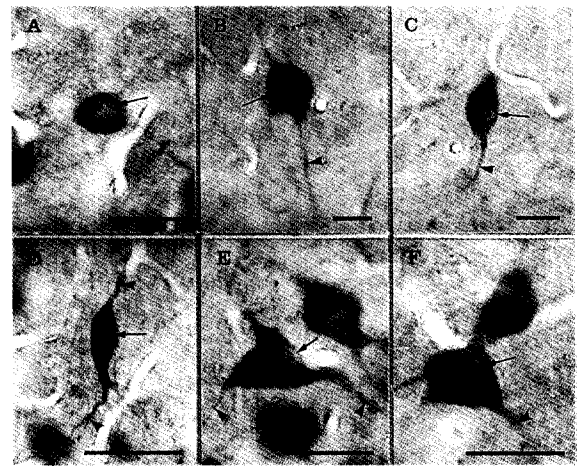


**Fig. 2.** Six ChAT-immunoreactive nerve cell types in the coronal sections of the PND 21 rat MCPO. The round (A), oval (B), elongated (C), fusiform (D), triangular (E), and polygonal (F) nerve cells with long dendrites (arrowheads) are seen. Arrows indicate non-immunoreactive nuclei in those cells. Scale bars=25 μm.

### *Frequency distributions of the ChAT-immunoreactive nerve cell types*

The ChAT-immunoreactive nerve cells could be classified into the round, oval, elongated, fusiform, triangular, and polygonal types according to the cell shape and the ratio of long axis versus short axis of the cell soma (Fig. 2). As shown in Table 1, the frequency distributions of the round (18.9%) and oval (67.6%) types were high in the PND 0 rats, while those of the elongated (30.1%) and fusiform (1.8%) types in the PND 35 rats and of the triangular (20.4%) and polygonal (17.4%) types were high in the adult rats. The frequency distribution of the oval type was higher than those of the other types, while the frequency distribution of the fusiform was very low compared to those of other types.

### *The volumes of ChAT-immunoreactive nerve cell somata and the differentiation of the neurites*

As shown in the Table 2 and Fig. 3, the soma volumes of the immunoreactive nerve cells progressively increased from PND 0 (1,832 $\mu m^3$) to PND 17 (4,983 $\mu m^3$) and thereafter they decreased to the level of adult (2,323 $\mu m^3$). The soma volume of the immunoreactive

**Table 1.** The frequency distributions of the ChAT-immunoreactive nerve cell types in the MCPO of the postnatal and adult rats

| Postnatal age (day) | Number of cells scored | Frequency distribution (%) of nerve cell types | | | | | | Total |
|---|---|---|---|---|---|---|---|---|
| | | Round | Oval | Elongated | Fusiform | Triangular | Polygonal | |
| 0 | 127 | 18.9 | 67.6 | 6.0 | 0.3 | 6.8 | 0.4 | 100 |
| 7 | 207 | 10.7 | 62.1 | 14.1 | 0.5 | 11.1 | 1.5 | 100 |
| 14 | 491 | 12.2 | 50.0 | 23.8 | 0.4 | 10.2 | 3.4 | 100 |
| 17 | 224 | 10.7 | 42.3 | 26.7 | 0.9 | 15.2 | 4.2 | 100 |
| 21 | 519 | 9.5 | 40.8 | 27.7 | 0.8 | 16.2 | 5.0 | 100 |
| 28 | 383 | 9.0 | 35.4 | 27.9 | 1.3 | 16.7 | 9.7 | 100 |
| 35 | 493 | 7.9 | 31.8 | 30.1 | 1.8 | 17.8 | 10.6 | 100 |
| 90 ± 10 | 425 | 5.2 | 28.0 | 27.7 | 1.3 | 20.4 | 17.4 | 100 |

**Table 2.** The cell soma volumes of the ChAT-immunoreactive nerve cell types in the MCPO of the postnatal and adult rats

| Postnatal age (d) | Number of cells scored | Cell soma volume ($\mu m^3$, mean±S.E.) of nerve cell types | | | | | | Mean |
|---|---|---|---|---|---|---|---|---|
| | | Round | Oval | Elongated | Fusiform | Triangular | Polygonal | |
| 0 | 127 | 2,168±191 | 1,857±108 | 2,217±191 | 1,925± 59 | 1,418±260 | 1,406± 72 | 1,832±147 |
| 7 | 207 | 2,944±124 | 2,565± 80 | 2,440±143 | 2,694± 20 | 2,817±218 | 1,967±269 | 2,571±142 |
| 14 | 419 | 5,184±254 | 4,529±103 | 4,284±135 | 3,123±119 | 4,602±292 | 3,289±347 | 4,169±208 |
| 17 | 224 | 5,983±507 | 5,126±194 | 4,808±174 | 3,186±904 | 5,018±282 | 4,029±402 | 4,983±245 |
| 21 | 519 | 4,024±233 | 3,461± 89 | 3,135± 98 | 2,052±382 | 3,831±176 | 2,803±181 | 3,218±193 |
| 28 | 383 | 3,417±200 | 3,390±105 | 3,040±103 | 2,015±430 | 3,791±197 | 2,369±171 | 3,004±201 |
| 35 | 493 | 3,358±189 | 3,048± 79 | 2,835± 78 | 2,800±465 | 2,965±131 | 2,105±121 | 2,852±140 |
| 90±10 | 425 | 2,704±123 | 2,433± 64 | 2,242± 96 | 2,103±399 | 2,152± 86 | 2,301±121 | 2,323±111 |

cell was shown to be the largest in the PND 17. The soma volumes of the round nerve cells were larger than those in the other cell types, except for the cases of the PND 0 and 28 rats, while those of the fusiform nerve cell were very small compared to other cell types.

One or two sproutings of neurites from the soma of the immunoreactive nerve cell in the PND 0-14 rats were frequently found (Fig. 3A-C). In the PND 21 (Fig. 2) and 28 (Fig. 3D) rats, it was observed that several typical neurites sprouted from the cell soma and increased in number.

*The cell soma volumes in each cell type*

As shown in the Fig. 4, the change of frequency distributions of cell soma volumes in six cell types at the developmental stages (e.g. PND 7 and 17) and the adult was investigated. The cell soma volumes increased with developmental age (from PND 7 to PND 17) and thereafter decreased progressively to the adult. Generally, the cell soma volumes in the round and oval types at the PND 7 and in all cell types, with the exception of the fusiform cell type, at the adult appeared to exhibit a unimodal distribution. But, at the PND 17, those in all cell types were evenly distributed as well as possessing a wide range.

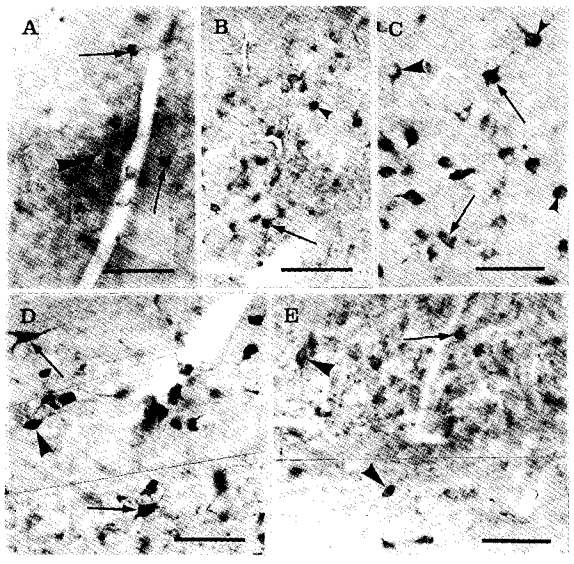


**Fig. 3.** Comparison of the sizes of ChAT-immunoreactive nerve cells in the MCPOs during postnatal development. A, Triangular (arrowhead) and polygonal (arrows) immunoreactive nerve cells with short dendrites in the PND 0 rat. B, Oval (arrowhead) and polygonal (arrow) nerve cells in the PND 7 rat. C, Oval (small arrowheads), elongated (large arrowhead) and polygonal (arrows) nerve cells in the PND 14 rat. D, Elongated (arrowhead) and polygonal (arrows) in the PND 28 rat. E, Oval (arrow) and elongated (arrowheads) cells in the adult rat. The sizes of immunoreactive nerve cells in the PND 0 and 7 are significantly smaller than those in the PND 14 and 28, whereas they are almost the same in size as those in the adult. Scale bars=100 μm.

*Electron microscopy for ChAT-immunoreactive nerve cells*

Immunoreactive nerve cells in the PND 21 rat forebrains were observed by electron microscope. The cell had a large nucleus with several indentations of nuclear envelope (Fig. 5A). Well developed Golgi complexes, mitochondria, RER, polysomes, and free ribosomes were found. Several axosomatic synapses on the cell membrane were detected (Fig. 5A and C). These axon terminals contained a few synaptic vesicles and mitochondria.

The free ribosomes, polysomes and RER of the nerve cells in the MCPO of PND 21 rat forebrains were identified to be ChAT-immunoreactive in the tissues untreated with Triton X-100, but Golgi complexes were non-immunoreactive.

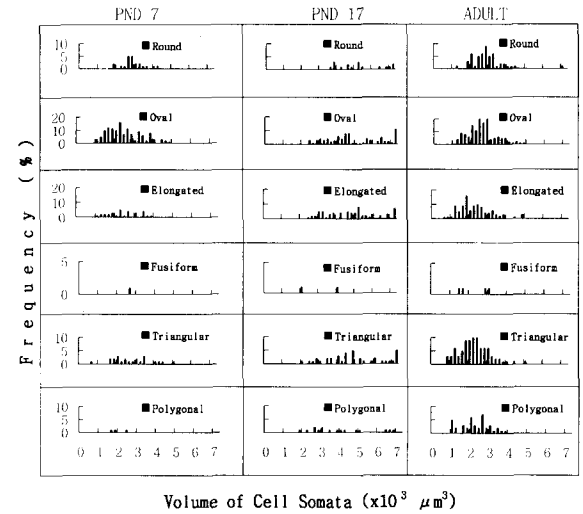


**Fig. 4.** Histograms illustrating the frequlncy distributions of the cell soma volumes ($\mu m^3$) of round, oval, elongated, fusiform, triangular, and polygonal cells in the MCPO of the PND 7, PND 17 and adult rat forebrains.

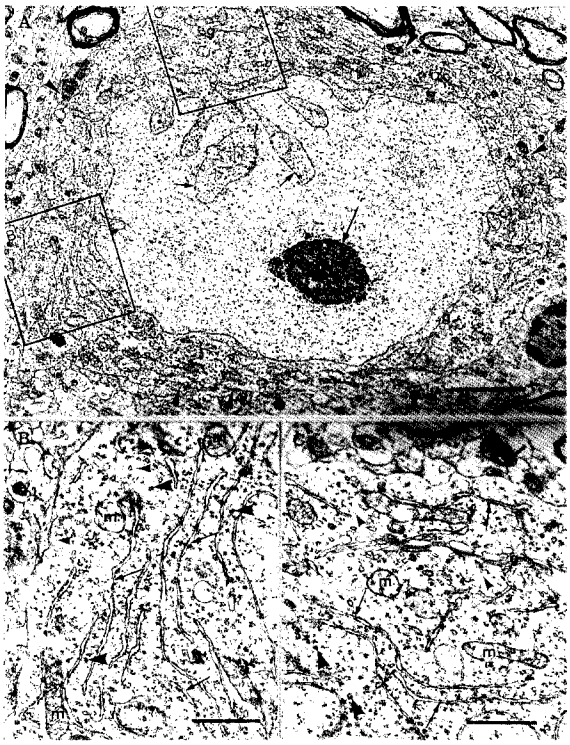

Fig. 5. Electron micrographs of the ChAT-immunoreactive nerve cells in the MCPO of the PND 21 rat forebrain at the anterior commisure. A, A immunoreactive nerve cell. This cell nucleus shows deep indentations (short arrows) and prominent nucleolus (long arrow). Especially, rough endoplasmic reticula, Golgi complexes (g), mitochondria (m), and ribosomes are well developed. Axosomatic synapses (arrow heads) are seen on the cell membrane. B and C, Enlarged parts from A. Immunoreactive free ribosomes (small arrowheads), polysomes (large arrowheads) and RER (arrows) are seen as well as the non-immuno-reactive Golgi complex (g). A axosomatic synapse (large arrow) is located on the cell membrane. Scale bars=1 μm (B, C) and 4 μm (A).

## Discussion

In the present investigation, many immunoreactive nerve cells lied intermingled within the longitudinal fibers of medial forebrain bundle, but these were shown to be more closed together in the intimate area to the caudal part of horizontal diagonal band of Broca as shown in Fig. 1E. Gritti et al. (1993) described that the cholinergic neurons in the MCPO of the rat lied in the course of the longitudinal fibers of the medial forebrain bundle and in continuity with those of the horizontal diagonadal band of Broca as well as resembling in their prominent size and multipolarity.

In this study, the immunoreactivities of the nerve cell cytoplasm in the PND 0 rat (Figs. 1A and 3A) were identified to be very weak. It progressively increased throughout postnatal development (Figs. 1-3). The above observations were identical with the findings of Gould et al. (1991) in the same nucleus of the rat and with the descriptions of Ko et al. (1995) in the medial septal nucleus and diagonal bands of Broca. But, the immunoreactivities in the basal nucleus of Meynert and caudate-putamen of the postnatal rats were first identified in the PND 7 and PND 10 rats, respectively (Gould et al., 1991). Therefore, it could be considered that the ChAT-immunoreactivities in the various nuclei of the postnatal rat forebrains could be variable and this variation may be related the level of tissue differentiation in the forebrain nuclei.

In the early postnatal rats (Figs. 1A and B, and 3A and B), the nerve fibers were not differentiated and also the immunoreactivity of the fibers was weak. But, during postnatal development the immunoreactivity of the nerve fibers was gradually increased. In the late postnatal stages (Figs. 1C and D, and 3C and D), it was relatively intense compared to that in the early postnatal stages. In the PND 35 (Fig. 1D) and the adult (Fig. 1E), the nerve fibers were shown to be well developed.

In the light microscopic observation, the intracellular immunoreactivity was almost even (Figs. 2 and 3). Such finding was identical with the phenomenon that the immunoreactive ribosomes, polysomes, and RER were evenly distributed in the cytoplasm on the electron microscopic observation (Fig. 5).

Dinopoulos (1988) classified the Golgi-impregnated neurons in the basal forebrain of the rat into three cell types on the basis of soma shape and dendritic form: 1) triangular, 2) round, and 3) fusiform types. But, in the previous studies (Chung et al., 1994; Ko et al. 1995), the nerve growth factor receptor-immunoreactive and the ChAT-immunoreactive nerve cells were classified in detail into six types in the other basal forebrain nuclei of the postnatal and adult rats on the basis of the cell shape and the ratio of long axis versus short axis of the cell soma. In this study, ChAT-immunoreactive nerve cells also could be classified into six cell types (Fig. 2). Thus, the changes of both frequency distributions of cell types and their soma volumes were examined during the developmental process (Tables 1 and 2 and Fig. 4).

Gould et al (1989) described that the somata and dendrites of the cholinergic neurons in the rat forebrain were changed during the postnatal development. Satoh et al. (1983) also observed the same neurons in the MCPO of adult rats in which the polygonal cells were increased in number. Those observations were similar to the finding in this study that the frequency distributions of triangular and polygonal cells increased throughout the progressive postnatal development. Consequently, it is considered that the nerve cells are differentiated into several cell types following the sprouting and development of the neurites throughout the postnatal developmental processes. Therefore, the frequency distributions of the differentiated cell types are progressively increased.

In the PND 0 rat of the present study, the total mean volumes of the immunoreactive nerve cell somata were the lowest (1,406-2,217 $\mu m^3$), while those in the PND 17 were the highest (3,186-5,983 $\mu m^3$).

Those were almost the same as the results of Gould et al. (1989) that the cross-sectional cell body areas progressively increase, peaking at postnatal day 18. In the PND 17 rats, the development of the neurites of nerve cells were predominant and the cell soma volumes were significantly increased (Table 1 and Fig. 4). The cell soma volumes of six cell types in the PND 17 rat were evenly distributed with a wide range. Such distributions were significantly different from a unimodal distribution of most cell types at the other developmental stage (e.g. PND 7) and the adult. It is supposed that the increase of cell soma in the PND 17 rat is an event of previous process for sprouting of neurites. Such distribution has not been observed previously in the rat forebrains. But, Gould et al. (1989) reported that the progressive increases were related in number of primary dendrities, number of dendritic branch points, and the length of the longest dendrite that peaked at PND 18 and thereafter decreased with the exception of dendritic length which monotonically increased until adulthood. Therefore, it is considered that the increase of cell volumes, the development of neurites, the morphological change of cell somata and the increase of frequency of the differentiated cell types in the MCPO during postnatal development are the inevitable processes of the differentiation of immunoreactive nerve cells.

The free ribosomes, polysomes, and RER of the nerve cells were immunoreactive in this electron microscopic observation (Fig. 5). In the median septum and diagonal band of Broca of the rat forebrain, Ko et al. (1995) also confirmed the same ChAT-immunoreactivity in the identical cell organelles. On the other hand, it was particularly interesting that the Golgi complexes were non-immunoreactive. Therefore, it is concluded that both the intracellular localization and the synthesis of ChAT correlate closely with the free ribosomes, polysomes and RER, but not with Golgi complexes.

#### Acknowledgments

This study was supported by a grant from Hallym University.

## References

Armstrong DM (1986) Ultrastructural characterization of choline acetyltransferase-containing neurons in the basal forebrain of rat: evidence for a cholinergic innervation of intracerebral blood vessels. *J Comp Neurol* 250: 81-92.

Armstrong DM, Saper CB, Levey AI, Wainer BH, and Terry RD (1983) Distribution of cholinergic neurons in the rat brain: demonstrated by the immunocytochemical localization of choline acetyltransferase. *J Comp Neurol* 216: 53-68.

Bayer SA and Altman J (1987) Development of the preoptic area: time and site of origin, migratory routes, and settling patterns of its neurons. *J Comp Neurol* 265: 69-95.

Brantley RK and Bass AH (1988) Cholinergic neurons in the brain of a teleost fish (*Polichthys notatus*) located with a monoclonal antibody to choline acetyltransferase. *J Comp Neurol* 275: 87-105.

Butcher LL, Oh JD, Woolf NJ, Edwards RH, and Roghani A (1992) Organization of central cholinergic neurons revealed by combined *in situ* hibridization histochemistry and choline-O-acetotransferase immunocytochemistry. *Neurochem Int* 21: 429-445.

Buzsaki G, Bickford RG, Ponomareff G, Thal LJ, Mandel R, and Gage FH (1988) Nucleus basalis and thalamic control of neocortical activity in the freely moving rat. *J Neurosci* 10: 4007-4026.

Chung YW, Hong YH, and Ko CY (1994) Immunohistochemical study on the nerve growth factor receptors in the basal forebrain nuclei of the postnatal and the adult rats. *Korean J Zool* 37: 385-408.

Ciani F, Franceschini V, and Del Grande P (1988) Histochemical and biochemical study on the acetylcholinesterase and choline acetyltransferase in the brain and spinal cord of frog, *Rana esculenta*. *J Hirnforsch* 29: 157-163.

Detari L and Vanderwolf CH (1987) Activity of identified cortically projecting and other basal forebrain neurones during large slow waves and cortical activation. *Brain Res* 437: 1-8.

Dinopoulos A, Parnavelas JG, Uylings HBM, and Van Eden CG (1988) Morphology of neurons in the basal forebrain nuclei of the rat: a Golgi study. *J Comp Neurol* 272: 461-474.

Drachman DA (1977) Memory and cognitive function in man: does the cholinergic system have a specific role? *Neurology* 27: 783-790.

Dreyfus CF, Bernd P, Martinez HJ, Rubin SJ, and Black IB (1989) GABAergic and cholinergic neurons exhibit high-affinity nerve growth factor binding in rat basal forebrain. *Exp Neurol* 104: 181-185.

Eckenstein F (1988) Transient expression of NGFreceptor-like immunoreactivity in postnatal rat brain and spinal cord. *Brain Res* 446: 149-154.

Gould E, Farris TW, and Butcher LL (1989) Basal forebrain neurons undergo somatal and dendritic remodeling during postnatal development: a single-section Golgi and choline acetyltransferase analysis. *Dev Brain Res* 46: 297-302.

Gould E, Woolf NJ, and Butcher LL (1991) Postnatal development of cholinergic neurons in rat. I. Forebrain. *Brain Res Bull* 27: 767-789.

Gritti I, Mainville L, and Jones BE (1993) Codistribution of GABA- with acetylcholine-synthesizing neurons in the basal forebrain of the rat. *J Comp Neurol* 329: 438-457.

Grove EA, Domesick VB, and Nauta WJH (1986) Light microscopic evidence of striatal input to intrapallidal neurons of cholinergic cell group Ch4 in the rat: a study employing the anterograde tracer *Phaseolus vulgaris* leucoagglutinin (PHA-L). *Brain Res* 367: 379-384.

Happe HK and Murrin LC (1992) Development of high-affinity choline transport sites in rat forebrain: a quantitative autoradiography study with [$^3$H] hemicholinium-3. *J Comp Neurol* 321: 591-611.

Hellweg R, Fisher W, Hock C, Gage FH, Bjoerklund A, and Thoenen H (1990) Nerve growth factor levels and choline acetyltransferase activity in the brain of aged rats with spatial memory impairments. *Brain Res* 537: 123-130.

Houser CR, Crawford GD, Barber RP, Salvaterra PM, and Vaughn JE (1983) Organization and morphological characteristics of cholinergic neurons: an immunocytochemical study with a monoclonal antibody to choline acetyltransferase. *Brain Res* 266: 97-119.

Hsu SM, Raine L, and Fanger H (1981) Use of avidin-biotin complex (ABC) in immunoperoxidase techniques: a comparison between ABC and unlabeled antibody (PAP) procedure. *J Histochem Cytochem* 29: 577-580.

Ko CY, Chung YW, and Hong YH (1995) Immunohistochemical study of the cholinergic nerve cells in the medial septal nucleus and diagonal band of Broca of the postnatal and adult rats. *Korean J Zool* 38: 248-268.

Koh S, Chang P, Collier TJ, and Loy R (1989) Loss of NGF receptor immunoreactivity in basal forebrain neurons of aged rats: correlation with spatial memory impairment. *Brain Res*

498: 397-404.
McGeer EG and McGeer PL (1981) Cholinergic mechanisms in central disorders. In: Palmore GC (ed), Neuropharmacology of Central Nerve System and Behavioral Disorders. Academic Press, New York, pp 479-505.
McGeer PL, Eccles JC, and McGeer EG (1987) Molecular Neurobiology of the Mammalian Brain. 2nd ed. Plenum Press, New York, pp 235-263.
McLean IW and Nakane PK (1974) Periodate-lysine-paraformaldehyde: a new fixative for immunoelectron microscopy. *J Histochem Cytochem* 122: 1077-1085.
Medina L, Smeets WJAJ, Hoogland PV, and Puelles L (1993) Distribution of choline acetyltransferase immunoreactivity in the brain of the lizard *Gallotia galloti*. *J Comp Neurol* 331: 261-285.
Mesulam MM, Mash D, Hersh L, Bothwell M, and Geula C (1992) Cholinergic innervation of human striatum, globus pallidus, subthalamic nucleus, substantia nigra, and red nucleus. *J Comp Neurol* 323: 252-268.
Oh JD, Woolf NJ, Roghani A, Edwards RH, and Butcher LL (1992) Cholinergic neurons in the rat central nerve system demonstrated by *in situ* hybridization of choline acetyltransferase mRNA. *Neuroscience* 47: 807-822.
Paxinos G and Watson C (1986) The Rat Brain in Stereotaxic Coordinate. 2nd ed. Academic Press, Sydney, pp 1-27.
Satoh K, Amstrong DM, and Fibiger HC (1983) A comparison of the distribution of central cholinergic neurons as demonstrated by acetylcholinesterase phamacohistochemistry and choline acetyltransferase immunohistochemistry. *Brain Res Bull* 11: 693-720.
Sofroniew MV, Pearson RCA, and Owell TPSP (1987) The cholinergic nuclei of the basal forebrain of the rat: normal structure, development and experimentally induced degeneration. *Brain Res* 411: 310-331.
Szymusiak R and McGinty D (1986) Sleep-related neuronal discharge in the basal forebrain of cats. *Brain Res* 370: 82-92.

[Received April 20, 1997; accepted June 12, 1997]